

# The Vibrational Spectra of the Boron Halides and Their Molecular Complexes. Part 14. *Ab Initio* Studies of the Boron Trifluoride-Nitrous Acid Complex

T. Anthony Ford

School of Chemistry and Physics, University of KwaZulu-Natal, Westville Campus, Private Bag X54001, Durban, 4000, South Africa.  
E-mail: [ford@ukzn.ac.za](mailto:ford@ukzn.ac.za)

Received 18 June 2013, accepted 29 July 2013.

## ABSTRACT

A number of electron donor-acceptor complexes formed between boron trifluoride and nitrous acid have been studied, in order to ascertain which of the interacting monomers acts as the acid and which as the base. We have found four complexes in which electron donation occurs in the direction  $\text{HONO} \rightarrow \text{BF}_3$ . These complexes are bound through the hydroxyl O, the N and the nitrosyl O atoms, in decreasing order of strength of interaction, and in the last case two separate rotational isomers have been identified. The intermolecular structural parameters and the perturbations of the intramolecular bond lengths and angles are consistent with the trends in the interaction energies. The vibrational spectra have also been examined, and the wavenumber shifts and intensity ratios track with the energetic and structural data. The mechanism of complex formation in each case is donation of a lone pair of electrons on the N or O atoms into the  $\pi^*$  orbital of  $\text{BF}_3$ , with back donation in the case of the complex bound through the nitrogen atom from a lone pair on one of the F atoms of  $\text{BF}_3$  into the  $\sigma^*(\text{OH})$  orbital of HONO. The total amounts of charge transferred vary, in general, with the strengths of interaction, while the charge density topologies and their properties confirm the conclusions derived from the other characteristics discussed.

## KEYWORDS

*Ab initio* studies, molecular complexes, boron trifluoride, nitrous acid.

## 1. Introduction

Boron trifluoride is a prototypical Lewis acid.<sup>1</sup> As such it is capable of forming a variety of electron donor-acceptor complexes with other small molecules. A survey of the standard databases reveals the wide range of complexes containing boron trifluoride which have been detected in the gas phase<sup>2,3</sup> and in cryogenic matrices.<sup>4,5</sup> Some of these complexes are listed in Tables S1 (gas phase species) and S2 (matrix isolated species) of the Supplementary Material. Complementary to the technique of matrix isolation spectroscopy in solid noble gas or nitrogen matrices is that of the use of cryogenic liquids (usually noble gases) as solvents for the examination of vibrational spectra. These studies have the advantage that they give direct experimental access to the enthalpies of reactions, which may be usefully compared with those derived from theoretical investigations. A number of such studies are listed in Table S3. A recent review of the vibrational properties of matrix isolated complexes of compounds formed from the main group elements lists a very comprehensive selection of adducts containing boron trifluoride.<sup>72</sup> In addition, a variety of theoretical computations of the properties of donor-acceptor complexes have been applied to a large number of associated species containing boron trifluoride. A selection of these complexes with neutral base species is listed in Table S4.

In a recent theoretical investigation, we employed *ab initio* molecular orbital theory to examine the complex formed between boron trifluoride and hydroxylamine.<sup>114</sup> This adduct is intriguing in that hydroxylamine presents two potential sites for electron

donation to the boron atom of the boron trifluoride molecule, the nitrogen and the oxygen atoms. We were interested to know which of these two interactions led to the more stable complex, what were the structures of the respective complexes and their relative energies of formation, and in what ways the vibrational spectra of the interacting monomers were perturbed as a result of the association. We concluded that the preferred complex involved primarily a  $\text{B}\dots\text{N}$  interaction, stabilized by a secondary weak, bent  $\text{OH}\dots\text{F}$  hydrogen bond, in a five-membered ring structure. Nitrous acid presents a further interesting example of a partner molecule in a complex with boron trifluoride, containing three potential competing sites of interaction with the boron atom, the nitrogen, the nitrosyl oxygen and the hydroxyl oxygen atoms. Nitrous acid itself has been shown to form a range of binary complexes, which have been detected mainly by matrix isolation spectroscopy, and Table S5 lists a number of these associated species, containing both the *cis* and *trans* isomers. In most of these adducts the nitrous acid molecule is the proton donor in a hydrogen-bonded structure, but in some cases it can act as an electron donor (e.g.  $\text{HF}$ ,<sup>126</sup>  $\text{HCl}$ ,<sup>126,127</sup>  $\text{SiH}_4$  and  $\text{GeH}_4$ ,<sup>137</sup>) and in others (e.g. formaldoxime<sup>140</sup> and allene<sup>141</sup>) as both. Some of these experimental studies have been supported by *ab initio* and DFT calculations.<sup>125–127,129,131–136,139–141</sup> In this paper we explore the structures and interaction energies of the possible structural forms of a 1:1 complex formed between boron trifluoride and nitrous acid, and examine the extent to which the vibrational spectra of the monomers are perturbed as a function of the strengths of interaction.

## 2. Computational Details

The calculations were carried out using the Gaussian-09 program,<sup>144</sup> at the second order level of Møller-Plesset perturbation theory (MP2)<sup>145</sup> and with Dunning's augmented correlation-consistent polarized valence triple-zeta basis set (aug-cc-pVTZ).<sup>146–150</sup> We optimized the structures of complexes of both the *trans* and *cis* HONO isomers, but in every case the *trans* structure was found to be more stable, and the *cis* complexes were therefore not considered further. Each structure was optimized and confirmed as a genuine energy minimum by the absence of any imaginary normal modes of vibration. The vibrational spectra were then recalculated at the anharmonic level. The computed interaction energies were corrected for basis set superposition error (BSSE)<sup>151</sup> by the Boys-Bernardi full counterpoise procedure<sup>152</sup> and for zero-point energy differences. In order to gain insight into the nature of the orbitals involved in the various interactions, the Natural Bond Orbital (NBO) approach was applied,<sup>153</sup> and further valuable information on the distribution of the charge densities and their topologies was derived using the Atoms-in-Molecules (AIM) formulation of Bader,<sup>154,155</sup> employing Keith's program AIMAll.<sup>156</sup>

## 3. Results and Discussion

### 3.1. Molecular Structures and Interaction Energies

In the complexes of *trans*-nitrous acid in which it functions as the electron donor, there is experimental evidence for the existence of three HF- or HCl-bonded species, with the diatomic acid proton interacting with all three available electron donor sites, although the preferred location is the hydroxyl oxygen atom.<sup>126,127</sup> In the complex with formaldoxime, the oxime OH group interacts with the nitrogen atom of HONO;<sup>140</sup> in the SiH<sub>4</sub> and GeH<sub>4</sub> adducts, the hydroxyl oxygen donates to the Si or Ge atom,<sup>137</sup> while in the complex with CH<sub>2</sub>=C=CH<sub>2</sub>,<sup>141</sup> in addition to the major OH...π bonded structure the nitrous acid molecule also accepts a secondary CH...N hydrogen bond. Thus all three electron-rich sites of nitrous acid are potential locations for interaction with the boron atom of BF<sub>3</sub>. We have examined all three possibilities. In the case of interaction with

**Table 1** Descriptions, symmetries and relative energies of the BF<sub>3</sub>.HONO complexes.

Structure	Conformation	Point group	Relative energy/kJ mol <sup>-1</sup>
1	cc <sup>a</sup>	C <sub>s</sub>	0
2	tc <sup>b</sup>	C <sub>1</sub>	0.76
3	ttt <sup>c</sup>	C <sub>s</sub>	6.56
4	tct <sup>d</sup>	C <sub>s</sub>	7.24

<sup>a</sup> cc refers to the *cis-cis* conformation with respect to the FBNOH chain.

<sup>b</sup> tc refers to the *trans-cis* conformation with respect to the FBNOH chain.

<sup>c</sup> ttt refers to the *trans-trans-trans* conformation with respect to the FBNOH chain.

<sup>d</sup> tct refers to the *trans-cis-trans* conformation with respect to the FBNOH chain.

the nitrosyl oxygen atom, two isomeric structures were found to be stationary points, which we have designated ttt and tct, referring to the *trans* or *cis* conformation with respect to the FBNOH atomic chain. Table 1 describes the structures and point groups of the resulting optimized adducts, and their minimized energies relative to the most stable isomer, while Fig. 1 represents the respective structures. The complexes in which the nitrogen and the nitrosyl oxygen atoms are the donor sites (**1**, **3** and **4**) feature a plane of symmetry, but that with the hydroxyl oxygen (**2**) has the hydrogen atom displaced from the pseudo-plane of the heavy atoms. The energies of structures **1** and **2** are fairly similar, but those bound through the nitrosyl oxygen (**3** and **4**) are noticeably less stable.

The interaction energies of the four complexes, appropriately corrected, are presented in Table 2. Consistent with the relative energies of the four structures, the interaction energies of **1** and **2** are a factor of 2 to 3 higher than those of **3** and **4**. The reversal of the order of the interaction energies of **1** and **2** relative to those in Table 1 is a consequence of a combination of the higher degree of distortion of the BF<sub>3</sub> bond lengths and angles as a result of the greater strain in the cyclic structure **1** and a greater zero-point energy difference for **1** than **2** (see later).

Table 3 reports the distortions of the geometrical parameters of the BF<sub>3</sub> and HONO fragments. The mean bond length and the mean unsigned bond angle changes of BF<sub>3</sub> are substantially greater for **1** and **2** than for the more weakly bound **3** and **4**. This

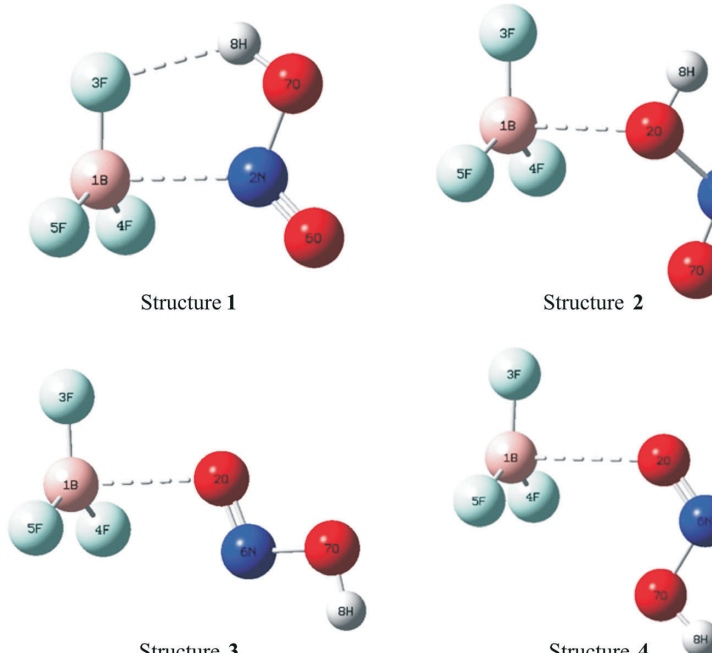


**Figure 1** Optimized structures of the four BF<sub>3</sub>.HONO complexes.

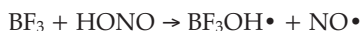
**Table 2** Interaction energies of the  $\text{BF}_3\text{-HONO}$  complexes, corrected for basis set superposition error and zero-point energy differences.

	Interaction energy/kJ mol <sup>-1</sup>			
	Structure 1	Structure 2	Structure 3	Structure 4
Uncorrected	-29.11	-28.89	-17.55	-16.21
Corrected <sup>a</sup>	-22.81	-23.59	-13.30	-12.13
Corrected <sup>b</sup>	-18.35	-22.72	-9.99	-8.97

<sup>a</sup> Corrected for BSSE only.<sup>b</sup> Corrected for BSSE and zero-point energy differences.**Table 3** Perturbations of the intramolecular geometrical parameters of the  $\text{BF}_3\text{-HONO}$  complexes.

Component	Parameter	Perturbation			
		Structure 1	Structure 2	Structure 3	Structure 4
$\text{BF}_3$	r(BF)/pm	1.91	0.89	0.14	0.21
		0.17	0.78	0.32	0.19
		0.17	0.22	0.32	0.19
	$\angle \text{FBF}/\text{deg}$	0.69	-0.64	-0.25	0.12
		-0.87	-0.22	-0.02	-0.16
		-0.87	-0.19	-0.02	-0.16
HONO	r(OH)/pm	0.33	0.10	0.07	0.05
	r(N-O)/pm	-3.72	6.66	-3.17	-2.55
	r(N=O)/pm	0.51	-1.59	1.03	0.85
	$\angle \text{HON}/\text{deg}$	0.54	0.27	0.41	0.57
	$\angle \text{ONO}/\text{deg}$	1.73	-0.49	-0.21	-0.02

is particularly true for **1**, due to the formation of the cyclic structure. In the case of the HONO fragment, the N-O bond experiences the greatest changes, increasing for structure **2**, but contracting in the other three adducts. In structure **2** the elongation of the N-O bond is accompanied by a shortening of the N=O bond, indicating a redistribution of charge within the ONO unit. The formation of this complex may represent an early stage in the reaction



The larger OH bond length and ONO angle changes for structure **1** are associated with the formation of the OH...F hydrogen bond. The intermolecular geometrical parameters are listed in Table 4. The separation of the boron atom from the site of electron donation, N or O, decreases monotonically with the strength of interaction, as shown in Fig. 2a, while the distortion of the  $\text{BF}_3$  unit from planarity, measured by the mean FB...N(O) angle, increases in the same order (Fig. 2b), confirming the link between the intermolecular structures and the interaction energies. In structures **1** and **2**, where the hydrogen atom approaches one of the fluorine atoms, the significantly shorter H...F distance and larger OH...F angle in **1** testify to the presence of an

OH...F hydrogen bond in this case, which is absent in structure **2**.

### 3.2. Vibrational Spectra

The effects of complexation on the anharmonic vibrational spectra of the interacting monomers are among the most reliable measures of the extent of interaction in molecular complexes. The computed spectra of the four complexes are available in the Supplementary Material in Tables S6 to S9. Table 5 shows the wavenumber shifts of the modes of the  $\text{BF}_3$  fragments in the four complexes studied. These shifts are almost exclusively to the red (the only two blue shifts being less than  $2 \text{ cm}^{-1}$ ). The most sensitive mode is the symmetric  $\text{BF}_3$  bending,  $\nu_2$ , as has been recognized by Young,<sup>72</sup> and the  $\nu_2$  wavenumber shifts correlate reasonably well with the interaction energies, as indicated in Fig. 3. Apart from complex **4**, the shifts of the symmetric stretching mode,  $\nu_1$ , are virtually independent of the structure. The antisymmetric stretching vibration,  $\nu_3$ , has two components due to the lifting of the degeneracy present in the uncomplexed  $\text{BF}_3$  monomer, and the shifts of this mode follow the behaviour of the  $\nu_2$  vibration. A large difference is observed between the shifts of the two components for structure **1**, as a consequence of the

**Table 4** Intermolecular geometrical parameters of the  $\text{BF}_3\text{-HONO}$  complexes.

Structure 1		Structure 2		Structure 3		Structure 4	
Parameter	Value	Parameter	Value	Parameter	Value	Parameter	Value
r(B...N)/pm	237.08	r(B...O)/pm	232.62	r(B...O)/pm	251.68	r(B...O)/pm	260.37
r(F...H)/pm	215.36	r(F...H)/pm	278.83	$\angle \text{FB...O}/\text{deg}$	91.26	$\angle \text{FB...O}/\text{deg}$	87.76
$\angle \text{BF...H}/\text{deg}$	104.90	$\angle \text{FB...O}/\text{deg}$	91.18	$\angle \text{B...ON}/\text{deg}$	110.74	$\angle \text{B...ON}/\text{deg}$	126.84
$\angle \text{FB...N}/\text{deg}$	88.08	$\angle \text{OH...F}/\text{deg}$	74.78				
$\angle \text{OH...F}/\text{deg}$	131.05	$\angle \text{B...OH}/\text{deg}$	113.34				
$\angle \text{ON...B}/\text{deg}$	113.18	$\angle \text{BF...H}/\text{deg}$	79.18				

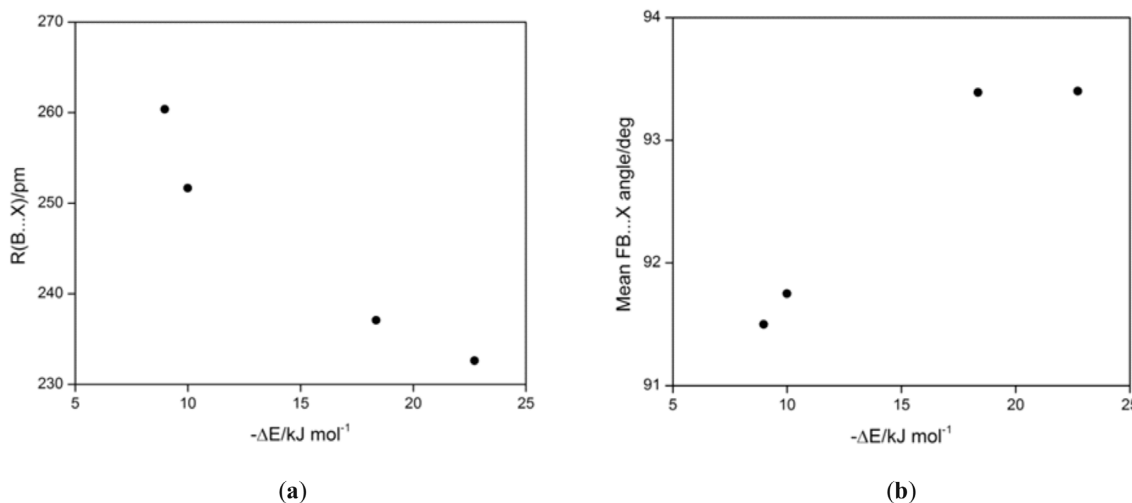


**Figure 2** Plots of (a) the  $\text{B}\dots\text{X}$  distance and (b) the mean  $\text{FB}\dots\text{X}$  angle *versus* the interaction energy of the four  $\text{BF}_3\text{-HONO}$  complexes ( $\text{X} = \text{N}, \text{O}$ ).

**Table 5** Intramolecular anharmonic wavenumber shifts of the  $\text{BF}_3$  fragments of the  $\text{BF}_3\text{-HONO}$  complexes.

Mode	Wavenumber shift/ $\text{cm}^{-1}$			
	Structure 1	Structure 2	Structure 3	Structure 4
$\nu_s(\text{BF}_3)$	-21.5	-20.4	-22.5	-7.2
$\delta_s(\text{BF}_3)$	-75.9	-88.3	-54.4	-29.7
$\nu_a(\text{BF}_3)$	-44.7 1.4	-36.1 -55.4	-7.8 -12.7	-10.9 -6.1
$\delta_a(\text{BF}_3)$	-2.5 -8.0	-7.5 -5.9	-0.6 -0.7	-1.8 1.1

decoupling of the in-plane and the out-of-plane BF stretching motions arising from the formation of the  $\text{OH}\dots\text{F}$  hydrogen bond. The shifts of the antisymmetric bending mode,  $\nu_a$ , are all less than  $10\text{ cm}^{-1}$ , particularly those of structures 3 and 4, and are not very useful in characterizing the alternative structures. In Table 6 are presented the corresponding wavenumber shifts of the HONO fragment modes, relative to the monomer. The  $\nu(\text{OH})$  vibration is regularly shifted to lower wavenumbers, with a larger red shift of  $\nu(\text{OH})$  in 1 than those of the other three complexes, characteristic of a genuinely hydrogen-bonded OH group. The  $\nu(\text{N}=\text{O})$  mode is also typically red-shifted, with generally larger perturbations than those of  $\nu(\text{OH})$ . The exception is structure 2, where  $\nu(\text{N}=\text{O})$  has a rather large blue shift.

Indeed, structure 2 is unique in that the remaining four modes all shift to lower wavenumber, while for complexes 1, 3 and 4 these modes are all perturbed to the blue. The unusual behaviour of 2 is attributed to its being bound through the hydroxyl oxygen atom, and Latajka *et al.*, on the basis of their matrix spectroscopic results, have identified this site as the most basic centre in the HONO molecule.<sup>126</sup> This finding is confirmed by the large red shifts of the ‘in-plane’ and ‘out-of-plane’ bending vibrations of the HON group,  $\delta(\text{HON})$  and  $\gamma(\text{HON})$ , which are by far the largest shifts among the four complexes. This observation is attributed to the fact that, although the hydroxyl hydrogen atom is not directly involved in the interaction, its motion is strongly coupled with that of the bound oxygen.

The symmetric stretching mode of the boron trifluoride monomer is, of course, infrared inactive, but it becomes activated on formation of the various complexes. The induced infrared activity of this mode is reported in Table 7. Although structures 1 and 2 are the most strongly bound of the four adducts, the degree of activation is greatest for 3 and 4. This is surprising, because the distortion of the  $\text{BF}_3$  molecule is least pronounced in the cases of 3 and 4, and the larger intensity enhancements must be due to the contribution of the nitrosyl oxygen atom in the mechanism of the binding process. The intensity ratios of the remaining modes of  $\text{BF}_3$  relative to the monomer are given in Table 8. For the  $\nu_2$  mode, complexation leads to an intensity enhancement. The antisymmetric stretching and bending modes,  $\nu_a(\text{BF}_3)$  and  $\delta_a(\text{BF}_3)$ , undergo intensity diminution on formation of the adducts, except for one of the components of  $\delta_a(\text{BF}_3)$  of structure 2, where the intensity increase is the largest for any mode of any complex. This is a consequence of the fact that in structure 2,

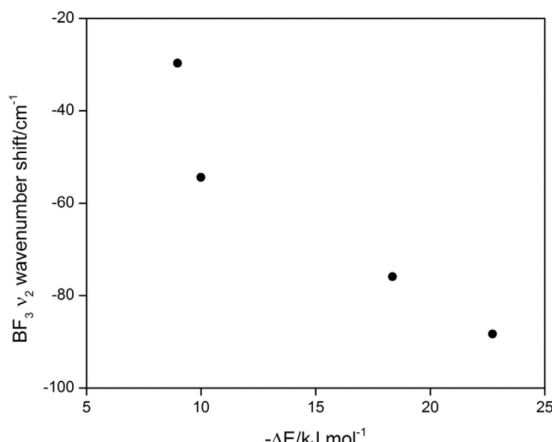


**Figure 3** Plot of the  $\nu_2$  wavenumber shift of the  $\text{BF}_3$  molecule *versus* the interaction energy of the four  $\text{BF}_3\text{-HONO}$  complexes.

**Table 6** Intramolecular anharmonic wavenumber shifts of the HONO fragments of the  $\text{BF}_3\text{-HONO}$  complexes.

Mode	Wavenumber shift/cm <sup>-1</sup>			
	Structure 1	Structure 2	Structure 3	Structure 4
$\nu(\text{OH})$	-38.5	-8.7	-7.4	-4.1
$\nu(\text{N}=\text{O})$	-28.0	71.7	-41.8	-38.5
$\delta(\text{HON})$	55.3	-98.9	31.0	20.3
$\nu(\text{N-O})$	47.0	-83.7	72.4	38.2
$\delta(\text{ONO})$	74.6	-16.2	90.5	54.0
$\gamma(\text{HON})$	39.6	-217.8	22.1	19.9

**Table 7** Infrared intensities of the symmetric stretching modes of the  $\text{BF}_3$  fragments of the  $\text{BF}_3\text{-HONO}$  complexes.

Structure	Intensity/km mol <sup>-1</sup>
1	8.98
2	7.44
3	87.24
4	11.78

both components of  $\delta_a(\text{BF}_3)$  belong to the same symmetry species, and there is considerable intensity borrowing between the two components. Table 9 lists the intensity ratios of the modes of the HONO fragments. These ratios are fairly unremarkable, except for the OH stretching and the in-plane HON bending modes in structure 1, which possesses a genuine hydrogen bond. The intensities of these two modes are enhanced to a greater extent than in the other three complexes, in accordance with normal observation for hydrogen-bonded complexes. The out-of-plane HON bending mode of structure 2 also suffers a large perturbation. This is because the hydroxyl oxygen atom is the site of interaction, and the proximity of the OH bond to the B electron acceptor site increases the OH bond polarity substantially.

### 3.3. Natural Bond Orbital Analysis

A natural bond orbital (NBO)<sup>153</sup> analysis was carried out to

determine which molecular orbitals of the interacting molecules were involved in the formation of the complexes, and to quantify the amount of charge transferred as a result of the interactions, per atom and per molecule. Table 10 shows the main interactions present in each structure, with their orbital interaction energies. An arbitrary cut-off of 5 kJ mol<sup>-1</sup> was applied to these interaction energies. The common feature of all these interactions is donation from a N or O lone pair orbital of the base into the  $\pi^*$  orbital of  $\text{BF}_3$  (essentially the vacant 2p orbital on boron). In the case of structure 1 there is also a secondary donation from the N lone pair to the  $\sigma^*(\text{BF})$  orbital associated with the BF bond lying in the symmetry plane. Unique to structure 1 is a back donation from an in-plane lone pair orbital of F3 to the  $\sigma^*(\text{OH})$  orbital of HONO. This back donation is responsible for the cyclic nature of structure 1. In structure 2 there are two interactions, of approximately equal importance, involving the lone pair orbitals of the hydroxyl oxygen. One is a virtually pure 2p O orbital and the other is a hybrid with almost equal s and p character. In structures 3 and 4 it is the nitrosyl oxygen atom which is responsible for the electron donation; in each case the dominant donor orbital is an almost pure 2p orbital, while a minor contribution comes from the hybrid O orbital having mostly s character.

The NBO analysis also gives an indication of the amount of charge redistribution occurring on complex formation. The net charge shift is exclusively in the direction  $\text{HONO} \rightarrow \text{BF}_3$ , and the total amount of charge transferred decreases in the order struc-

**Table 8** Complex/monomer infrared intensity ratios of the  $\text{BF}_3$  fragments of the  $\text{BF}_3\text{-HONO}$  complexes.

Mode	Intensity ratio			
	Structure 1	Structure 2	Structure 3	Structure 4
$\delta_s(\text{BF}_3)$	2.63	1.16	3.70	1.12
$\nu_a(\text{BF}_3)$	0.52	0.89	0.89	0.89
	0.89	0.88	0.91	0.90
$\delta_a(\text{BF}_3)$	0.66	5.78	0.84	0.66
	0.36	0.50	0.82	0.94

**Table 9** Complex/monomer infrared intensity ratios of the HONO fragments of the  $\text{BF}_3\text{-HONO}$  complexes.

Mode	Intensity ratio			
	Structure 1	Structure 2	Structure 3	Structure 4
$\nu(\text{OH})$	1.63	1.07	1.33	1.27
$\nu(\text{N}=\text{O})$	0.79	1.51	0.87	0.84
$\delta(\text{HON})$	1.97	0.69	1.21	1.00
$\nu(\text{N-O})$	1.05	0.33	0.80	1.02
$\delta(\text{ONO})$	0.40	0.80	0.05	0.93
$\gamma(\text{HON})$	0.84	2.91	0.99	1.00

**Table 10** Major molecular orbitals involved in the formation of the  $\text{BF}_3\text{-HONO}$  complexes, according to the NBO procedure. See Fig. 1 for numbering of the atoms.

Structure	HONO $\rightarrow \text{BF}_3$		$\text{BF}_3 \rightarrow \text{HONO}$	
	Interaction <sup>a</sup>	Interaction energy/kJ mol <sup>-1</sup>	Interaction	Interaction energy/kJ mol <sup>-1</sup>
<b>1</b>	n(N2) $\rightarrow \pi^*(\text{B1})$ n(N2) $\rightarrow \sigma^*(\text{B1F3})$	84.89 5.86	n(F3) $\rightarrow \sigma^*(\text{O7H8})$	5.27
<b>2</b>	n2(O2) $\rightarrow \pi^*(\text{B1})$ n1(O2) $\rightarrow \pi^*(\text{B1})$	35.61 32.47		
<b>3</b>	n2(O2) $\rightarrow \pi^*(\text{B1})$ n1(O2) $\rightarrow \pi^*(\text{B1})$	29.62 6.74		
<b>4</b>	n2(O2) $\rightarrow \pi^*(\text{B1})$ n1(O2) $\rightarrow \pi^*(\text{B1})$	11.00 9.96		

<sup>a</sup> n1 of oxygen atom O2 is a non-bonding hybrid orbital with 59.8 % s and 40.2 % p (structure 2), 69.1 % s and 30.9 % p (structure 3) and 70.5 % s and 29.4 % p character (structure 4), while n2 of oxygen atom O2 is a non-bonding hybrid orbital with 1.3 % s and 98.7 % p (structure 2), 2.2 % s and 97.6 % p (structure 3) and 0.5 % s and 99.3 % p character (structure 4).

ture **1** > structure **2** > structure **3** > structure **4**, as shown in Table 11. Only in structure **1** does the boron atom experience an increase of negative charge, as a result of the back donation effect. The fluorine atoms all accumulate negative charge, most notably the in-plane fluorine atoms in **1** and **2**. It is in the HONO fragment that the greatest discrimination among the four complexes becomes apparent. In each case the donor atom undergoes an increase of negative charge, with the hydroxyl O of **2** being most affected, followed by the N atom of **1** and the nitrosyl O atoms of **3** and **4**, correlating with the order of interaction energies (see Table 2). The hydrogen atoms of the HONO fragments consistently lose negative charge, again tracking with the order of the interaction energies.

#### 3.4. Atoms-in-Molecules Analysis

The application of Bader's Atoms-in-Molecules (AIM) theory,<sup>154,155</sup> implemented in Keith's AIMAll program,<sup>156</sup> provides further insight into the ways in which the monomer molecules interact in order to form the complexes. Molecular graphs of the four complexes are presented in Fig. 4, showing the bond paths and critical points, represented by small green dots. These graphs indicate that bond critical points are found in all the covalent bond regions, and in the intermolecular bonding regions (B1...N2 and F3...H8 in **1**, and B1...O2 in **2**, **3** and **4**). In addition, a ring critical point, indicated by a small red dot, is found in **1**, enclosed by the B1, N2, O7, H8 and F3 atoms, confirming the cyclic nature of this complex. The properties of the critical points associated with the covalent bond interactions, specifically the

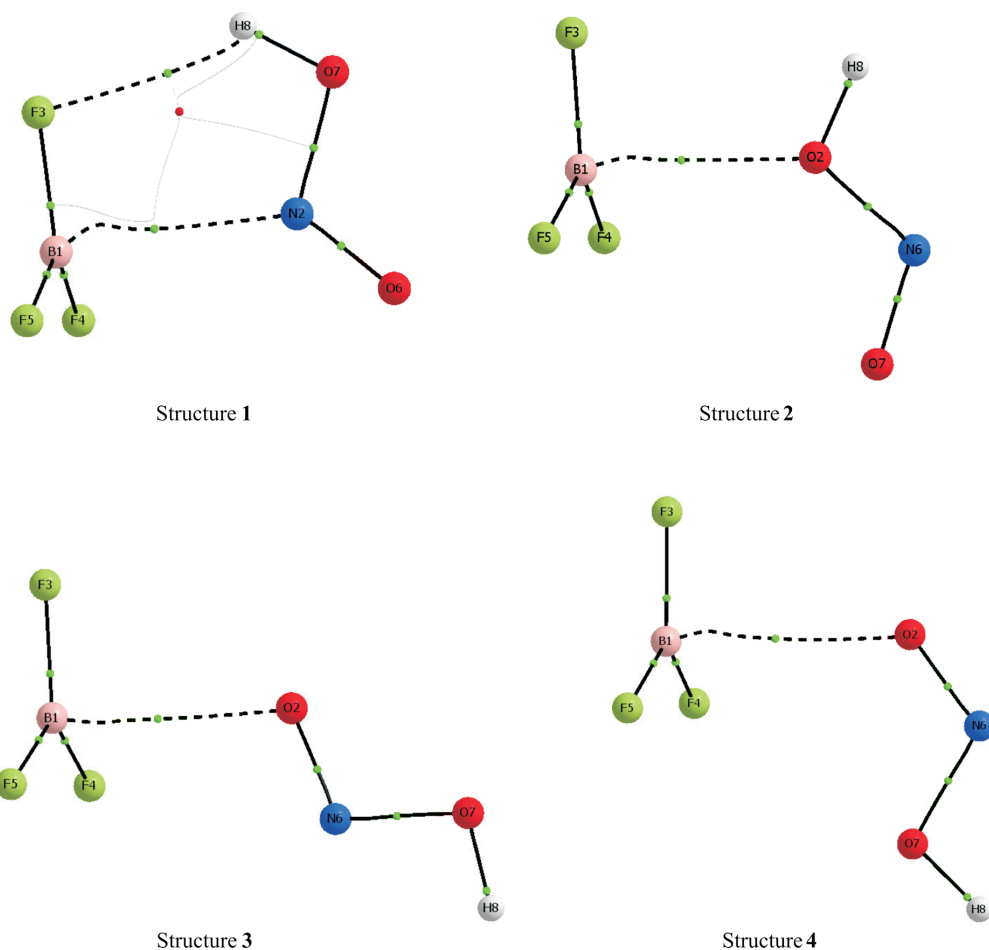
electron density,  $\rho_c$ , its Laplacian,  $\nabla^2\rho_c$ , the bond ellipticity,  $\varepsilon_c$ , the potential and kinetic energy densities,  $V_c$  and  $G_c$ , their sum,  $H_c$ , and the modulus of their ratio,  $|V_c/G_c|$ , are collected in Table 12. For the intermolecular interactions the values of these quantities are reported in Table 13. A number of generalizations have been observed for some of these properties.<sup>157–161</sup> For example, values of  $\rho_c > 0.1$  a.u. are characteristic of covalent bonds, where there is an accumulation of charge in the interatomic region, while for hydrogen bonds and van der Waals interactions,  $\rho_c$  is typically of the order of 0.01 a.u.<sup>157</sup> Table 12 shows that  $\rho_c$  for the N=O, OH, N-O and BF bonds falls off in that order, reflecting the relative bond strengths, while Table 13 indicates that the  $\rho_c$  values for the B...N and B...O bonds in structures **1** and **2**, which are the most strongly bound complexes, are noticeably higher than those of the other intermolecular interactions, although the values all fall within the appropriate range for such interactions. Also,  $\nabla^2\rho_c < 0$  for shared interactions and  $> 0$  for closed-shell interactions.<sup>158</sup> These conditions are certainly fulfilled by the entries for N=O, OH and N-O in Table 12 and those for B...N, B...O and F...H in Table 13. However,  $\nabla^2\rho_c > 0$  for the BF bonds, indicating a marked weakening of those bonds brought about by the molecular interactions and, curiously, also for the N-O bond in structure **2**. We can offer no explanation for this anomaly. The bond ellipticity,  $\varepsilon_c$ , approximates zero for covalent bonds, as shown in Table 12, but increases substantially for the intermolecular bonds (Table 13) where, again, the values for the B...N and B...O interactions in **1** and **2** are significantly greater than for those in structures **3** and **4**. Cremer and Kraka

**Table 11** NBO charge shifts of the atoms resulting from formation of the complexes, and total intermolecular charge transfers.

Atom	Amount of charge transferred/me			
	Structure 1	Structure 2	Structure 3	Structure 4
B	-6.6	13.6	9.4	10.3
F3	-27.7	-17.1 <sup>a</sup>	-5.8	-7.0
F4,F5	-4.4	-15.1 <sup>b</sup> , -7.6 <sup>b</sup>	-9.5	-7.1
Total $\text{BF}_3$	-43.1	-26.2	-15.4	-10.9
O (nitrosyl)	28.7	52.2	-45.9	-43.4
N	-47.1	34.6	21.3	21.2
O (hydroxyl)	38.9	-71.9	32.2	24.9
H	22.4	11.4	7.8	8.1
Total HONO	42.9	26.3	15.4	10.8

<sup>a</sup> Atom F3 is that closest to the B1O2...H8 plane.

<sup>b</sup> Atoms F4 and F5 are those straddling the B1O2...H8 plane.

**Figure 4** Molecular graphs of the four  $\text{BF}_3\text{-HONO}$  complexes**Table 12** Properties of the covalent bond critical points of the  $\text{BF}_3\text{-HONO}$  complexes.

Structure	Bond	$\rho_c/\text{a.u.}^a$	$\nabla^2\rho_c/\text{a.u.}^b$	$\varepsilon_c$	$V_c/\text{a.u.}^c$	$G_c/\text{a.u.}^c$	$H_c/\text{a.u.}^c$	$ V_c/G_c $
1	$\text{BF}_3$	0.1995	1.1932	0.0416	-0.6042	0.4512	-0.1530	1.3391
	$\text{BF}_4, \text{BF}_5$	0.2107	1.2778	0.0260	-0.6531	0.4863	-0.1668	1.3430
	$\text{N}=\text{O}$	0.5626	-1.7278	0.0904	-1.4088	0.4884	-0.9204	2.8845
	$\text{N}-\text{O}$	0.3283	-0.2542	0.1151	-0.5388	0.2376	-0.3012	2.2677
	$\text{OH}$	0.3546	-2.6488	0.0192	-0.8088	0.0733	-0.7355	11.0341
2	$\text{BF}_3$	0.2061	1.2425	0.0333	-0.6328	0.4717	-0.1411	1.3415
	$\text{BF}_4$	0.2068	1.2483	0.0322	-0.6358	0.4739	-0.1619	1.3416
	$\text{BF}_5$	0.2103	1.2764	0.0275	-0.6515	0.4853	-0.1662	1.3425
	$\text{N}=\text{O}$	0.5929	-2.0353	0.0702	-1.5941	0.5427	-1.0514	2.9374
	$\text{N}-\text{O}$	0.2529	0.0619	0.0973	-0.3644	0.1899	-0.1745	1.9189
	$\text{OH}$	0.3560	-2.6168	0.0193	-0.8090	0.0774	-0.7316	10.4522
3	$\text{BF}_3$	0.2105	1.2830	0.0246	-0.6534	0.4871	-0.1663	1.3414
	$\text{BF}_4, \text{BF}_5$	0.2093	1.2753	0.0262	-0.6481	0.4835	-0.1646	1.3404
	$\text{N}=\text{O}$	0.5552	-1.7153	0.0945	-1.3820	0.4766	-0.9054	2.8997
	$\text{N}-\text{O}$	0.3237	-0.2448	0.1097	-0.5274	0.2331	-0.2943	2.2625
	$\text{OH}$	0.3582	-2.6567	0.0202	-0.8149	0.0754	-0.7395	10.8077
4	$\text{BF}_3$	0.2101	1.2806	0.0247	-0.6516	0.4859	-0.1657	1.3410
	$\text{BF}_4, \text{BF}_5$	0.2101	1.2829	0.0244	-0.6517	0.4862	-0.1655	1.3404
	$\text{N}=\text{O}$	0.5574	-1.7345	0.0939	-1.3941	0.4802	-0.9139	2.9032
	$\text{N}-\text{O}$	0.3185	-0.2153	0.1095	-0.5147	0.2305	-0.2842	2.2330
	$\text{OH}$	0.3582	-2.6566	0.0199	-0.8152	0.0755	-0.7397	10.7974

<sup>a</sup> 1 a.u. of  $\rho_c = 1.0812 \times 10^{12} \text{ C m}^{-3}$ .<sup>b</sup> 1 a.u. of  $\nabla^2\rho_c = 3.8611 \times 10^{32} \text{ C m}^{-5}$ .<sup>c</sup> 1 a.u. of  $V_c, G_c$  and  $H_c = 1.7718 \times 10^{34} \text{ kJ mol}^{-1} \text{ m}^{-3}$ .

**Table 13** Properties of the intermolecular bond critical points of the  $\text{BF}_3\text{-HONO}$  complexes.

Structure	Bond	$\rho_c/\text{a.u.}^a$	$\nabla^2\rho_c/\text{a.u.}^b$	$\varepsilon_c$	$V_c/\text{a.u.}^c$	$G_c/\text{a.u.}^c$	$H_c/\text{a.u.}^c$	$ V_c/G_c $
<b>1</b>	B1...N2	0.0250	0.0572	0.6467	-0.0195	0.0169	-0.0026	1.1538
	F3...H8	0.0138	0.0619	0.3495	-0.0108	0.0131	0.0023	0.8244
	F3B1...N2O7H8...F3 <sup>d</sup>	0.0126	0.0634	-	-0.0109	0.0134	0.0025	0.8134
<b>2</b>	B1...O2	0.0220	0.0627	0.5722	-0.0173	0.0165	-0.0008	1.0485
<b>3</b>	B1...O2	0.0149	0.0504	0.3338	-0.0104	0.0115	0.0011	0.9043
<b>4</b>	B1...O2	0.0122	0.0434	0.4933	-0.0081	0.0095	0.0014	0.8526

<sup>a</sup> 1 a.u. of  $\rho_c = 1.0812 \times 10^{12} \text{ C m}^{-3}$ .<sup>b</sup> 1 a.u. of  $\nabla^2\rho_c = 3.8611 \times 10^{32} \text{ C m}^{-5}$ .<sup>c</sup> 1 a.u. of  $V_c$ ,  $G_c$  and  $H_c = 1.7718 \times 10^{34} \text{ kJ mol}^{-1} \text{ m}^{-3}$ .<sup>d</sup> Ring critical point.

have shown that  $|V_c| > G_c$  and  $H_c < 0$  for shared interactions, and  $|V_c| < G_c$  and  $H_c > 0$  for closed shell situations.<sup>159</sup> The relationships for the B...N and B...O interactions in Table 13 are consistent with this observation, except for the values of  $H_c$  for **1** and **2**, where the signs confirm the marked difference between the interaction energies of these two complexes and the others, as pointed out above. Finally,  $|V_c/G_c|$  has been shown to be typically  $< 1$  for closed shell interactions,  $> 2$  for shared interactions, and between 1 and 2 for intermediate cases.<sup>161</sup> The results given in Tables 12 and 13, by and large, confirm these expectations.

#### 4. Conclusions

Four distinct electron donor-acceptor complexes between  $\text{BF}_3$  and HONO have been identified, bound through the hydroxyl O, the N and the nitrosyl O atoms, in decreasing order of strength of interaction. The first two of these adducts are substantially more strongly bound than the other two. The perturbations of the intramolecular structural parameters, and the values of the intermolecular geometrical properties mirror these trends. The wavenumbers of the  $\text{BF}_3$  fragment modes vary in sensitivity to the degree of complexation, with the symmetric  $\text{BF}_3$  bending mode undergoing the largest shifts, in common with previous experience. The red shift of the OH stretching mode of HONO in structure **1** is considerably greater than those of the other complexes, consistent with the presence of an intermolecular hydrogen bond in this case. The mechanism of complex formation in each adduct is donation of a lone pair on N (structure **1**) or O (structures **2**, **3** and **4**) into the  $\pi^*$  orbital of  $\text{BF}_3$ , with back donation in the case of **1** from a lone pair on the in-plane F atom of  $\text{BF}_3$  into the  $\sigma^*(\text{OH})$  orbital of HONO. The total amounts of charge transferred track, in general, with the strengths of interaction, while the charge density topologies and their properties ratify the conclusions derived from the other characteristics discussed.

#### Acknowledgements

This work is based on research supported in part by the National Research Foundation of South Africa (NRF) under Grant No. 2053648. The grantholder acknowledges that opinions, findings and conclusions or recommendations expressed in any publication generated by NRF-supported research are those of the author and that the NRF accepts no liability in this regard. The author also acknowledges the University of KwaZulu-Natal Research Fund for financial assistance, and the Centre for High Performance Computing for the use of computing facilities.

#### References

- N.N. Greenwood and R.L. Martin, *Quart. Rev. Chem. Soc.*, 1954, **8**, 1–39.

- S.E. Novick, Bibliography of Rotational Spectra of Weakly Bound Complexes (2012). [https://wesfiles.wesleyan.edu/home/snovick/sn\\_webpage/vdw.pdf](https://wesfiles.wesleyan.edu/home/snovick/sn_webpage/vdw.pdf). Accessed 17 January 2013.
- J. Vogt and N. Vogt, *J. Mol. Structure*, 2004, **695**, 237–241.
- D.W. Ball, Z.H. Kafafi, L. Fredin, R.H. Hauge and J.L. Margrave, *A Bibliography of Matrix Isolation Spectroscopy, 1954–1985*, Rice University Press, Houston, TX, 1988.
- D.W. Ochsner, D.W. Ball and Z.H. Kafafi, *A Bibliography of Matrix Isolation Spectroscopy, 1985–1997*, Naval Research Laboratory Report No. NRL/PU/5610-98-357, Naval Research Laboratory, Washington, DC, July 1998.
- Y. Matsumoto, Y. Ohshima, M. Takami and K. Kuchitsu, *J. Chem. Phys.*, 1989, **90**, 7017–7021.
- G.-H. Lee, Y. Matsuo, M. Takami and Y. Matsumoto, *J. Chem. Phys.*, 1992, **96**, 4079–4087.
- K.C. Janda, L.S. Bernstein, J.M. Steed, S.E. Novick and W. Klemperer, *J. Am. Chem. Soc.*, 1978, **100**, 8074–8079.
- J.A. Phillips, M. Canagaratna, H. Goodfriend, A. Grushow, J. Almlöf and K.R. Leopold, *J. Am. Chem. Soc.*, 1995, **117**, 12549–12556.
- K. Nauta, R.E. Miller, G.T. Fraser and W.J. Lafferty, *Chem. Phys. Letters*, 2000, **322**, 401–406.
- J.M. LoBue, J.K. Rice, T.A. Blake and S.E. Novick, *J. Chem. Phys.*, 1986, **85**, 4261–4268.
- G.-H. Lee and M. Takami, *J. Chem. Phys.*, 1993, **98**, 3612–3619.
- G.-H. Lee and M. Takami, *J. Mol. Structure*, 1995, **352–353**, 417–422.
- T. Pradeep, C.S. Sreekanth and C.N.R. Rao, *J. Chem. Phys.*, 1989, **90**, 4704–4708.
- T. Pradeep and C.N.R. Rao, *J. Mol. Structure – Theochem.*, 1989, **200**, 339–352.
- S.W. Reeve, W.A. Burns, E.J. Lovas, R.D. Suenram and K.R. Leopold, *J. Phys. Chem.*, 1993, **97**, 10630–10637.
- D.L. Fiacco, Y. Mo, S.W. Hunt, M.E. Ott, A. Roberts and K.R. Leopold, *J. Phys. Chem. A*, 2001, **105**, 484–493.
- E.R.T. Kerstel, B.H. Pate, T.F. Mentel, X. Yang and G. Scoles, *J. Chem. Phys.*, 1994, **101**, 2762–2771.
- K.R. Leopold, G.T. Fraser and W. Klemperer, *J. Am. Chem. Soc.*, 1984, **106**, 897–899.
- M.C. Durrant, M.S. Hegde and C.N.R. Rao, *J. Chem. Phys.*, 1986, **85**, 6356–6360.
- T. Pradeep, C.S. Sreekanth, M.S. Hegde and C.N.R. Rao, *Chem. Phys. Letters*, 1988, **151**, 499–502.
- S.A. Peebles, L. Sun, R.L. Kuczkowski, L.M. Nxumalo and T.A. Ford, *J. Mol. Structure*, 1998, **471**, 235–242.
- A.C. Legon and H.E. Warner, *J. Chem. Soc., Chem. Commun.*, 1991, 1397–1399.
- D. Fujiang, P.W. Fowler and A.C. Legon, *J. Chem. Soc., Chem. Commun.*, 1995, 113–114.
- J.D. Odom, V.F. Kalasinsky and J.R. Durig, *Inorg. Chem.*, 1975, **14**, 2837–2839.
- B.J. van der Veken and E.J. Sluyts, *J. Phys. Chem. A*, 1997, **101**, 9070–9076.

- 27 W.A. Herrebout, A.A. Stolov and B.J. van der Veken, *J. Mol. Structure*, 2001, **563–564**, 221–226.
- 28 M.A. Dvorak, R.S. Ford, R.D. Suenram, F.J. Lovas and K.R. Leopold, *J. Am. Chem. Soc.*, 1992, **114**, 108–115.
- 29 I.H. Hillier, M.A. Vincent, J.A. Connor, M.F. Guest, A.A. MacDowell and W. von Niessen, *J. Chem. Soc., Faraday Trans. 2*, 1988, **84**, 409–415.
- 30 P.S. Bryan and R.L. Kuczkowski, *Inorg. Chem.*, 1971, **10**, 200–201.
- 31 J. Gebicki and J. Liang, *J. Mol. Structure*, 1984, **117**, 283–286.
- 32 L.M. Nxumalo and T.A. Ford, Proc. 9th International Conference on Fourier Transform Spectroscopy, (J.E. Bertie and H. Wieser, eds.), *Proc. SPIE*, 1993, **2089**, 200–201.
- 33 L.M. Nxumalo and T.A. Ford, *S. Afr. J. Chem.*, 1995, **48**, 30–38.
- 34 L.M. Nxumalo and T.A. Ford, *J. Mol. Structure*, 1997, **436–437**, 69–80.
- 35 L.M. Nxumalo and T.A. Ford, *Spectrochim. Acta*, 1997, **53A**, 2511–2524.
- 36 R.L. Hunt and B.S. Ault, *Spectrosc. Intern. J.*, 1982, **1**, 45–61.
- 37 D.W. Ball and M.J. Zehe, NASA Technical Memorandum No. 106422, 1993.
- 38 D.G. Evans, G.A. Yeo and T.A. Ford, *Faraday Discuss. Chem. Soc.*, 1988, No. 86, 55–64.
- 39 M.E. Jacox, K.K. Irikura and W.E. Thompson, *J. Chem. Phys.*, 2000, **113**, 5705–5715.
- 40 L.M. Nxumalo and T.A. Ford, *J. Mol. Structure*, 2003, **661–662**, 153–159.
- 41 J.M. Bassler, P.L. Timms and J.L. Margrave, *J. Chem. Phys.*, 1966, **45**, 2704–2706.
- 42 F.M.M. O'Neill, G.A. Yeo and T.A. Ford, *J. Mol. Structure*, 1988, **173**, 337–348.
- 43 L.M. Nxumalo and T.A. Ford, *Vibr. Spectrosc.*, 1994, **6**, 333–343.
- 44 R.L. Hunt and B.S. Ault, *Spectrosc. Intern. J.*, 1982, **1**, 31–44.
- 45 L.M. Nxumalo, M. Andrzejak and T.A. Ford, *Vibr. Spectrosc.*, 1996, **12**, 221–235.
- 46 N.P. Wells and J.A. Phillips, *J. Phys. Chem. A*, 2002, **106**, 1518–1523.
- 47 R. Hattori, E. Suzuki and K. Shimizu, *J. Mol. Structure*, 2005, **750**, 123–134.
- 48 A.A. Eigner, J.A. Rohde, C.C. Knutson and J.A. Phillips, *J. Phys. Chem. B*, 2007, **111**, 1402–1407.
- 49 I.R. Beattie and P.J. Jones, *Angew. Chem. Intern. Edit. Engl.*, 1996, **35**, 1527–1529.
- 50 R. Hattori, E. Suzuki and K. Shimizu, *J. Mol. Structure*, 2005, **738**, 165–170.
- 51 W.A. Herrebout, J. Lundell and B.J. van der Veken, *J. Phys. Chem. A*, 1998, **102**, 10173–10181.
- 52 L.M. Nxumalo and T.A. Ford, *Mikrochim. Acta [Suppl.]*, 1997, **14**, 383–385.
- 53 L.M. Nxumalo and T.A. Ford, *J. Mol. Structure*, 2003, **656**, 303–319.
- 54 R.R. Knauf, H.M. Helminiaik, J.P. Wrass, T.M. Gallert and J.A. Phillips, *J. Phys. Org. Chem.*, 2012, **25**, 493–501.
- 55 J.A. Phillips, D.J. Giesen, N.P. Wells, J.A. Halfen, C.C. Knutson and J.P. Wrass, *J. Phys. Chem. A*, 2005, **109**, 8199–8208.
- 56 D.W. Ball, M.J. Zehe and W. Morales, *Tribol. Trans.*, 2000, **43**, 767–773.
- 57 W.A. Herrebout and B.J. van der Veken, *J. Am. Chem. Soc.*, 1998, **120**, 9921–9929.
- 58 E.J. Sluyts and B.J. van der Veken, *J. Am. Chem. Soc.*, 1996, **118**, 440–445.
- 59 B.J. van der Veken and E.J. Sluyts, *J. Mol. Structure*, 1995, **349**, 461–464.
- 60 B.J. van der Veken, E.J. Sluyts and W.A. Herrebout, *J. Mol. Structure*, 1998, **449**, 219–229.
- 61 A.A. Stolov, W.A. Herrebout and B.J. van der Veken, *J. Am. Chem. Soc.*, 1998, **120**, 7310–7319.
- 62 W.A. Herrebout, J. Lundell and B.J. van der Veken, *J. Mol. Structure*, 1999, **480–481**, 489–493.
- 63 W.A. Herrebout, J. Lundell and B.J. van der Veken, *J. Phys. Chem. A*, 1999, **103**, 7639–7645.
- 64 W.A. Herrebout and B.J. van der Veken, *J. Am. Chem. Soc.*, 1997, **119**, 10446–10454.
- 65 W.A. Herrebout and B.J. van der Veken, *Phys. Chem. Chem. Phys.*, 1999, **1**, 3445–3452.
- 66 G.P. Everaert, W.A. Herrebout and B.J. van der Veken, *Spectrochim. Acta*, 2005, **61A**, 1375–1387.
- 67 G.P. Everaert, W.A. Herrebout, B.J. van der Veken, J. Lundell and M. Räsänen, *Chem. Eur. J.*, 1998, **4**, 321–327.
- 68 W.A. Herrebout, R. Szostak and B.J. van der Veken, *J. Phys. Chem. A*, 2000, **104**, 8480–8488.
- 69 W.A. Herrebout and B.J. van der Veken, *J. Mol. Structure*, 2000, **550–551**, 389–398.
- 70 G.P. Everaert, W.A. Herrebout and B.J. van der Veken, *J. Phys. Chem. A*, 2001, **105**, 9058–9067.
- 71 W.A. Herrebout, A. Gatin, G.P. Everaert, A.I. Fishman and B.J. van der Veken, *Spectrochim. Acta*, 2005, **61A**, 1431–1444.
- 72 N.A. Young, *Coord. Chem. Rev.*, 2013, **257**, 956–1010.
- 73 T.A. Ford, *Spectrochim. Acta*, 2005, **61A**, 1403–1409.
- 74 S. Fau and G. Frenking, *Mol. Phys.*, 1999, **96**, 519–527.
- 75 A. Garcia-Leigh and J.N. Murrell, *Croat. Chem. Acta*, 1984, **57**, 879–886.
- 76 L.M. Nxumalo, M. Andrzejak and T.A. Ford, *J. Chem. Inf. Comput. Sci.*, 1996, **36**, 377–384.
- 77 W.A. Herrebout and B.J. van der Veken, *J. Am. Chem. Soc.*, 1998, **120**, 9921–9929.
- 78 L.M. Nxumalo, M. Andrzejak and T.A. Ford, *J. Mol. Structure*, 1999, **509**, 287–295.
- 79 G.A. Yeo and T.A. Ford, *J. Mol. Structure – Theochem*, 2006, **771**, 157–164.
- 80 E. Silla, E. Scrocco and J. Tomasi, *Theoret. Chim. Acta*, 1975, **40**, 343–348.
- 81 G. Alagona, E. Scrocco, E. Silla and J. Tomasi, *Theoret. Chim. Acta*, 1977, **45**, 127–136.
- 82 A. Arnau, J. Bertran and E. Silla, *J. Chem. Soc., Perkin Trans. 2*, 1989, 509–512.
- 83 G. Scholz, *J. Mol. Structure – Theochem*, 1994, **309**, 227–234.
- 84 D. Kim and M.L. Klein, *Chem. Phys. Letters*, 1999, **308**, 235–241.
- 85 D.T. Clark, B.J. Cromarty and A. Sgamellotti, *Chem. Phys.*, 1980, **46**, 43–52.
- 86 W.L. Luken, B.A.B. Seiders and G.A. Blake, *Chem. Phys.*, 1985, **92**, 255–262.
- 87 V.M. Rayón and J.A. Sordo, *J. Phys. Chem. A*, 1997, **101**, 7414–7419.
- 88 L.M. Nxumalo, G.A. Yeo and T.A. Ford, *Theoret. Chem. Accounts*, 1997, **96**, 157–165.
- 89 V. Jonas, G. Frenking and M.T. Reetz, *J. Am. Chem. Soc.*, 1994, **116**, 8741–8753.
- 90 Y. Hase, *J. Mol. Structure – Theochem*, 1987, **151**, 223–226.
- 91 E. Iglesias, T.L. Sordo and J.A. Sordo, *Chem. Phys. Letters*, 1996, **248**, 179–181.
- 92 E.M. Cabaleiro-Lago and M.A. Ríos, *Chem. Phys. Letters*, 1998, **294**, 272–276.
- 93 J.A. Phillips and C.J. Cramer, *J. Chem. Theory Comput.*, 2005, **1**, 827–833.
- 94 L.M. Nxumalo, G.A. Yeo and T.A. Ford, *S. Afr. J. Chem.*, 1998, **51**, 25–34.
- 95 A. Rauk, I.R. Hunt and B.A. Kemp, *J. Org. Chem.*, 1994, **59**, 6808–6816.
- 96 D.W. Ball, *J. Mol. Structure – Theochem*, 1995, **331**, 223–228.
- 97 B.D. Rowsell, R.J. Gillespie and G.L. Heard, *Inorg. Chem.*, 1999, **38**, 4659–4662.
- 98 G.A. Yeo and T.A. Ford, *S. Afr. J. Chem.*, 2006, **59**, 129–134.
- 99 T.A. Ford, *J. Mol. Structure*, 2007, **834–836**, 30–41.
- 100 R. Jurgens and J. Almlöf, *Chem. Phys. Letters*, 1991, **176**, 263–265.
- 101 L.M. Nxumalo and T.A. Ford, *J. Mol. Structure*, 1993, **300**, 325–338.
- 102 L.M. Nxumalo and T.A. Ford, *J. Mol. Structure – Theochem*, 1995, **357**, 59–65.
- 103 F. Hirota, K. Miyata and S. Shibata, *J. Mol. Structure – Theochem*, 1989, **201**, 99–101.
- 104 V. Jonas and G. Frenking, *J. Chem. Soc., Chem. Commun.*, 1994, 1489–1490.
- 105 H. Anane, A. Boutalib, I. Nebot-Gil and F. Tomás, *J. Phys. Chem. A*, 1998, **102**, 7070–7073.
- 106 F. Gaffoor and T.A. Ford, *Spectrochim. Acta*, 2008, **71A**, 550–558.

- 107 T.A. Ford and D. Steele, *J. Phys. Chem.*, 1996, **100**, 19336–19343.
- 108 R. Ahlrichs, M.R. Bar, M. Häser and E. Sattler, *Chem. Phys. Letters*, 1991, **184**, 353–358.
- 109 T.A. Ford, *J. Phys. Chem. A*, 2008, **112**, 7296–7302.
- 110 V. Branchadell and A. Oliva, *J. Am. Chem. Soc.*, 1991, **113**, 4132–4136.
- 111 T.A. Ford, *Intern. J. Quantum Chem.*, 2012, **112**, 478–488.
- 112 T.J. LePage and K.B. Wiberg, *J. Am. Chem. Soc.*, 1988, **110**, 6642–6650.
- 113 T.A. Ford, *J. Mol. Structure*, 2009, **897**, 145–148.
- 114 T.A. Ford, *S. Afr. J. Chem.*, 2008, **61**, 74–81.
- 115 N.J. Fitzpatrick and M.O. Fanning, *J. Mol. Structure*, 1978, **50**, 127–132.
- 116 D.J. Giesen and J.A. Phillips, *J. Phys. Chem. A*, 2003, **107**, 4009–4018.
- 117 J.A. Phillips, J.A. Halfen, J.P. Wrass, C.C. Knutson and C.J. Cramer, *Inorg. Chem.*, 2006, **45**, 722–731.
- 118 B.W. Gung and M.A. Wolf, *J. Org. Chem.*, 1992, **57**, 1370–1375.
- 119 F. Hirota, Y. Koyama and S. Shibata, *J. Mol. Structure*, 1981, **70**, 305–307.
- 120 L.M. Nxumalo and T.A. Ford, *J. Mol. Structure – Theochem*, 1996, **369**, 115–126.
- 121 W. Morales, *J. Mol. Structure – Theochem*, 1997, **391**, 225–230.
- 122 J.A. Phillips, D.J. Giesen, N.P. Wells, J.A. Halfen, C.C. Knutson and J.P. Wrass, *J. Phys. Chem. A*, 2005, **109**, 8199–8208.
- 123 K. Sato, Y. Sakuma, S. Iwabuchi and H. Hirai, *J. Polymer Sci. A*, 1992, **30**, 2011–2015.
- 124 Z. Mielke, T. Talik and K.G. Tokhadze, *J. Mol. Structure*, 1999, **484**, 207–214.
- 125 Z. Mielke, Z. Latajka, J. Kołodziej and K.G. Tokhadze, *J. Phys. Chem.*, 1996, **100**, 11610–11615.
- 126 Z. Latajka, Z. Mielke, A. Olbert-Majkut, R. Wieczorek and K.G. Tokhadze, *Phys. Chem. Chem. Phys.*, 1999, **1**, 2441–2448.
- 127 A. Pieretti, N. Sanna, A. Hallou, L. Schriver-Mazzuoli and A. Schriver, *J. Mol. Structure*, 1998, **447**, 223–233.
- 128 Z. Mielke, A. Olbert-Majkut and K.G. Tokhadze, *J. Chem. Phys.*, 2003, **118**, 1364–1377.
- 129 Z. Mielke, Z. Latajka, A. Olbert-Majkut and R. Wieczorek, *J. Phys. Chem. A*, 2000, **104**, 3764–3769.
- 130 M. Wierzejewska and M. Dziadosz, *J. Mol. Structure*, 1999, **513**, 155–167.
- 131 A. Olbert-Majkut, Z. Mielke and K.G. Tokhadze, *Chem. Phys.*, 2002, **280**, 211–227.
- 132 M. Wierzejewska, Z. Mielke, R. Wieczorek and Z. Latajka, *Chem. Phys.*, 1998, **228**, 17–29.
- 133 M. Wierzejewska and A. Olbert-Majkut, *J. Phys. Chem. A*, 2003, **107**, 10944–10952.
- 134 A. Olbert-Majkut, Z. Mielke, R. Wieczorek and Z. Latajka, *Intern. J. Quantum Chem.*, 2002, **90**, 1140–1150.
- 135 M. Krajewska, A. Olbert-Majkut and Z. Mielke, *Phys. Chem. Chem. Phys.*, 2002, **4**, 4305–4313.
- 136 Z. Mielke, K.G. Tokhadze, Z. Latajka and E. Ratajczak, *J. Phys. Chem.*, 1996, **100**, 539–545.
- 137 Z. Mielke and K.G. Tokhadze, *Chem. Phys. Letters*, 2000, **316**, 108–114.
- 138 M. Krajewska, Z. Mielke and K.G. Tokhadze, *J. Mol. Structure*, 1997, **404**, 47–53.
- 139 A. Olbert-Majkut and Z. Mielke, *Chem. Phys.*, 2006, **324**, 689–698.
- 140 B. Golec, A. Bil and Z. Mielke, *J. Phys. Chem. A*, 2009, **113**, 9434–9441.
- 141 M. Krajewska, Z. Latajka, Z. Mielke, K. Mierzwicki, A. Olbert-Majkut and M. Sałdyka, *J. Phys. Chem. B*, 2004, **108**, 15578–15586.
- 142 M. Wierzejewska, *J. Mol. Structure*, 2000, **520**, 199–214.
- 143 Z. Mielke, M. Wierzejewska, A. Olbert, M. Krajewska and K.G. Tokhadze, *J. Mol. Structure*, 1997, **436–437**, 339–347.
- 144 M.J. Frisch, G.W. Trucks, H.B. Schlegel, G.E. Scuseria, M.A. Robb, J.R. Cheeseman, G. Scalmani, V. Barone, B. Mennucci, G.A. Petersson, H. Nakatsuji, M. Caricato, X. Li, H.P. Hratchian, A.F. Izmaylov, J. Bloino, G. Zheng, J.L. Sonnenberg, M. Hada, M. Ehara, K. Toyota, R. Fukuda, J. Hasegawa, M. Ishida, T. Nakajima, Y. Honda, O. Kitao, H. Nakai, T. Vreven, J.A. Montgomery, Jr., J.E. Peralta, F. Ogliaro, M. Bearpark, J.J. Heyd, E. Brothers, K.N. Kudin, V.N. Staroverov, R. Kobayashi, J. Normand, K. Raghavachari, A. Rendell, J.C. Burant, S.S. Iyengar, J. Tomasi, M. Cossi, N. Rega, J.M. Millam, M. Klene, J.E. Knox, J.B. Cross, V. Bakken, C. Adamo, J. Jaramillo, R. Gomperts, R.E. Stratmann, O. Yazyev, A.J. Austin, R. Cammi, C. Pomelli, J.W. Ochterski, R.L. Martin, K. Morokuma, V.G. Zakrzewski, G.A. Voth, P. Salvador, J.J. Dannenberg, S. Dapprich, A.D. Daniels, O. Farkas, J.B. Foresman, J.V. Ortiz, J. Cioslowski and D.J. Fox, *Gaussian-09, Revision A.02*, Gaussian, Inc., Wallingford, CT, 2009.
- 145 C. Møller and M.S. Plesset, *Phys. Rev.*, 1934, **46**, 618–622.
- 146 T.H. Dunning, Jr., *J. Chem. Phys.*, 1989, **90**, 1007–1023.
- 147 R.A. Kendall, T.H. Dunning, Jr. and R.J. Harrison, *J. Chem. Phys.*, 1992, **96**, 6796–6806.
- 148 D.E. Woon and T.H. Dunning, Jr., *J. Chem. Phys.*, 1993, **98**, 1358–1371.
- 149 K.A. Peterson, D.E. Woon and T.H. Dunning, Jr., *J. Chem. Phys.*, 1994, **100**, 7410–7415.
- 150 A. Wilson, T. van Mourik and T.H. Dunning, Jr., *J. Mol. Structure – Theochem*, 1997, **388**, 339–349.
- 151 B. Liu and A.D. McLean, *J. Chem. Phys.*, 1973, **59**, 4557–4558.
- 152 S.F. Boys and F. Bernardi, *Mol. Phys.*, 1970, **19**, 553–556.
- 153 A.E. Reed, L.A. Curtiss and F. Weinhold, *Chem. Rev.*, 1988, **88**, 899–926.
- 154 R.F.W. Bader, *Atoms in Molecules – A Quantum Theory*, Clarendon Press, Oxford, 1990.
- 155 R.F.W. Bader, *Chem. Rev.*, 1991, **91**, 893–928.
- 156 T.A. Keith, AIMAll, Version 11.03.14, 1997–2011. (<http://aim.tkristmill.com>, accessed 23 March 2011).
- 157 R.F.W. Bader, *J. Phys. Chem. A*, 1998, **102**, 7314–7323.
- 158 R.F.W. Bader and H. Essen, *J. Chem. Phys.*, 1984, **80**, 1943–1960.
- 159 D. Cremer and E. Kraka, *Angew. Chem. Intern. Edit. Engl.*, 1984, **23**, 627–628.
- 160 U. Koch and P.L.A. Popelier, *J. Phys. Chem.*, 1995, **99**, 9747–9754.
- 161 E. Espinosa, I. Alkorta, J. Elguero and E. Molins, *J. Chem. Phys.*, 2002, **117**, 5529–5542.